Absolute Detection and Collisional Destruction of 2.5-keV Metastable Hydrogen Atoms Produced by a Charge-Exchange Process in Cesium Vapor

G. Spiess, A. Valance, and P. Pradel
Service de Physique Atomique, Centre d'Etudes Nucleaires de Saclay, Gif-sur-Yvette, France
(Received 21 January 1972)

We have studied a near-resonant charge-exchange process between incident protons and a cesium vapor target. The cross section σ_{+0} for the production of all the neutral states of hydrogen decreases slightly with increasing energy. It varies from $(10 \pm 3) \times 10^{-15}$ cm^2 at 0.5 keV to $(6.4 \pm 1.6) \times 10^{-15}$ cm^2 at 2.5 keV. The cross section σ_{+m} for the production of the $2S_{1/2}$ metastable state of hydrogen is $(1.7 \pm 0.6) \times 10^{-15}$ cm^2 at 2.4 keV. The percentage of metastable atoms in the outgoing neutral beam is found to be 0.27 ± 0.08 for cesium target thickness less than 10^{13} atoms/cm^2. The outgoing fraction of $H(2S_{1/2})$ atoms reaches a maximum equal to 0.13 for a cesium thickness of 1.2×10^{14} atoms/cm^2. The collisional quenching processes studied are the electron loss of $H(2S_{1/2})$ on the noble gases H_2, N_2, and HI at 2.5 keV and the electron attachment of $H(2S_{1/2})$ on N_2 at the same energy. The electron-loss cross sections σ_{m+}, in units of 10^{-16} cm^2, and known with a 35% uncertainty, are 4.1 for He, 2.7 for Ne, 2.9 for Ar, 2.7 for Kr, 6 for Xe, 3.4 for H_2, and 5 for N_2. The cross section σ_{m+} is always greater than σ_{g+}, the electron-loss cross section for the ground state of hydrogen. The maximum ratio 9.7 of these two cross sections is obtained with the halogen compound target HI, which is an interesting gas to selectively ionize $H(2S_{1/2})$ in a beam containing the two species $H(2S_{1/2})$ and $H(1S_{1/2})$. A comparison of the data is made with theoretical predictions using an impulse approximation. Attachment cross sections of $H(2S_{1/2})$ and $H(1S_{1/2})$ have been measured on N_2 at 2.5 keV. We obtain $\sigma_{m-} = (1.2 \pm 0.4) \times 10^{-16}$ cm^2 and $\sigma_{g-} = (9.7 \pm 2) \times 10^{-18}$ cm^2.

I. INTRODUCTION

Metastable hydrogen atoms $H(2S_{1/2})$ are of interest in all media where excitation energy is present, such as electrical discharges, reentry shock waves, the upper atmosphere of the earth and the planets, stellar atmospheres, and so on. An important application to nuclear physics is the production of intense polarized H^- and H^+ ion beams, respectively, by electron attachment and electron loss of $H(2S)$ on an appropriate and selective target gas.

In spite of the recent increasing amount of investigation on collisional processes involving fast metastable hydrogen atoms, the experimental and theoretical results are still far from complete.

In this paper, we have chosen an efficient mechanism to produce an intense $H(2S)$ beam, first proposed by Donnally.[1] It is the near-resonant charge-exchange process between fast protons and cesium vapor. Cesium is the most suitable alkaline metal in the keV energy range as the small energy defect of the process

$$H^+ + Cs \rightarrow H(2S_{1/2}) + Cs^+ - 0.49 \text{ eV}$$

ensures a large cross section σ_{+m} for production of metastable atoms.

Two radiative states of hydrogen, $2P_{1/2}$ and $2P_{3/2}$, are also produced with nearly the same energy defect, so that the cross section σ_{+m} is a fraction F of the total charge-exchange cross section σ_{+0} for production of all the neutral states $n = 2$ of hydrogen.

In our experiment, absolute measurements of σ_{+0}, σ_{+m}, and F are performed at 2.5 keV and comparisons are made with previous results.[1-4]

To detect the metastable atoms, advantage is taken of the low value of the Lamb shift. An applied electric field mixes the metastable and radiative states with $n = 2$ by the Stark effect, inducing a quenching transition with the subsequent emission of a Lyman-α photon which is detected by a calibrated channeltron sensitive to ultraviolet. Furthermore, Ott *et al.*[5] have shown that the Lyman-α emission is polarized with regard to the electric field direction, and Sellin *et al.*[6] and Crandall[7] have predicted a dependence of the polarization with the electric field strength.

When the percentage F of metastable atoms in the outgoing neutral beam is known, it is possible to study in detail the collisional destruction of $H(2S)$ on atomic and molecular target gases.

The dominant destructive mechanisms in the keV energy range are electron loss,

$$H(2S) + X \rightarrow H^+ + X + e \quad (\sigma_{m+}),$$

electron attachment,

$$H(2S) + X \rightarrow H^- + X^+ \quad (\sigma_{m-}),$$

and deexcitation,

$$H(2S) + X \rightarrow H(1S) + X + \text{Ly-}\alpha \quad (\sigma_{mg}).$$

The metastable destruction cross section $\sigma_{m+} + \sigma_{m-} + \sigma_{mg}$ is known, although incorrectly, as the total

quenching cross section and was measured by Dose *et al.*[8] for collisions with Ar, N_2, and H_2O in the energy range 2–60 keV. Krotkov *et al.*[9,10] have also measured this cross section in a lower energy range (0.25–30 keV) for collisions with He and Ar.

Byron and Gersten[11] have shown that the total quenching cross section is mainly due to the deexcitation process at energies lower than 0.3 keV. They used an impact-parameter treatment and calculated the interaction potentials between H(2S) and He by a second-order perturbation theory compared with a semiempirical method of pseudopotentials including polarization effects. The theoretical cross section agrees well with the low-energy measurements of Krotkov. Levy[12] calculated the total quenching cross section for collisions with He, Ne, Ar, and Kr over the incident energy range 1 keV–1.6 MeV in the first Born approximation with the added approximation of closure used to describe target excitation. For incident energies above 4 keV, it is predicted that the electron-loss process dominates in the total quenching cross section. Gilbody *et al.*[13] measured, in the energy range 10–30 keV, the total quenching cross section and the electron-loss cross section for collisions with H_2, He, Ne, Ar, Kr, and N_2. Assuming that the attachment process is negligible above 10 keV, they calculated the difference to obtain the deexcitation cross section. It is found that the deexcitation process dominates the electron-loss process for H_2, Ne, Ar, and Kr in this energy range.

A theory of electron loss in the energy range 1–500 keV was developed by Bates and Walker[14,15] by using a classical impulse approximation. Comparison with the results of Gilbody *et al.* shows a good quantitative agreement for Ne and He and an energy-dependence agreement for the others gases.

Bell and Kingston[16] used a first Born approximation for the electron-loss process in collisions with H and He for energies above 5 keV. An energy-dependence agreement is found with the results of Gilbody *et al.* The electron-attachment process has been studied by Donnally and Sawyer[17] in argon and is important for the production of a polarized H^- ion beam. Recently, Kass and Williams[18] measured the total quenching cross section in collisions with He in the thermal-energy region. Agreement within 25% is obtained with Byron's theory. Finally, Baragiola and Salvatelli[19] have shown that the deexcitation process is perhaps the dominant process at 5-keV energy for Ne.

In this paper, measurements of the electron-loss cross section are reported at 2.5 keV for the following target gases: He, Ne, Ar, Kr, Xe, H_2, and N_2. Data are relative to the ground-state electron-loss cross section σ_{g+} measured by Williams,[20] except for N_2, for which the measurements are absolute. Comparisons are made with extrapolated experimental values of Gilbody *et al.* and with the theory of Bates.

An experiment undertaken in our laboratory for the purpose of obtaining a source of polarized protons is the electron-loss collision with HI, which is a favorable target gas for selective ionization because its electron energy affinity is close to the ionization energy of the metastable hydrogen atom. Previous results have been obtained by Brückman *et al.*[21,22] and Knutson[23] on I_2.

Finally we present an absolute measurement of the electron-attachment cross section for N_2 at 2.5 keV.

II. APPARATUS

A. General Description

A schematic diagram of the apparatus is shown in Fig. 1. A hydrogen-ion beam is extracted from a duoplasmatron source and is focused by an einzel lens. It is magnetically mass analyzed and is suitably collimated.

The proton beam enters a cell containing a

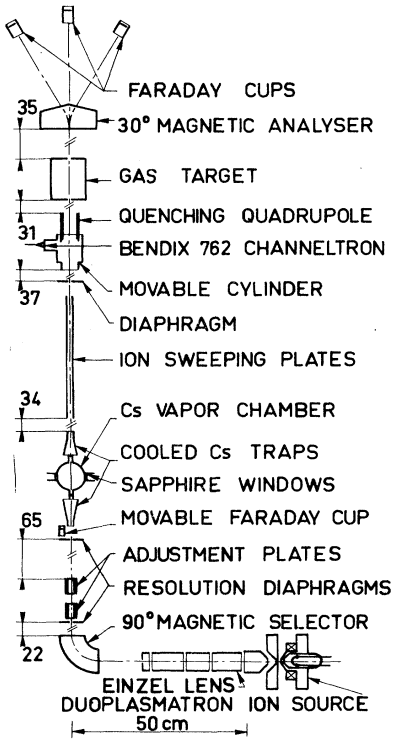

FIG. 1. Schematic diagram of the apparatus. All the chambers are drawn to scale. The spaces between them are indicated in cm on the figure. Five diffusion pumps maintain a pressure about 10^{-7} Torr. The Faraday cups are connected to Cary or Lemouzy electrometers. The gas cell is filled by means of a gas leak valve.

cesium vapor target with a thickness Π_{Cs} where quasiresonant charge-exchange processes occur.

The radiative $2P$ states decay essentially immediately while the $2S_{1/2}$ metastable state has a long lifetime (0.15 sec). The incident proton beam intensity I_+^0 at the entrance of the cell is measured by a movable Faraday cup. After the cell the entire beam passes through a drift region where the ions are swept away without destroying the metastable atoms. The metastable atom flux is determined by means of an electrostatic quench field where the Lyman-α photons, emitted by the Stark quenched metastable-atoms effect, are detected with a channeltron sensitive in the ultraviolet, and are counted.

A second cell, which contains a selected gas target X, is used to study the collisional-destruction processes of the metastable atoms. After the cell is a magnetic mass analyzer and three Faraday cups which are used to measure the ion intensities.

When the second gas cell is not filled and when no field is applied to the sweeping plates, the same Faraday cups can be used to measure the charge-exchange products which result from the passage of the primary proton beam through the cesium cell.

The experiment is performed with a vacuum system equipped with five trapped oil diffusion pumps. The pressure is approximately 10^{-7} Torr. The magnetic field caused by passing a suitable current through a coil wound on a long rectangular frame surrounding the entire apparatus is used to compensate the earth's magnetic field along the beam axis.

B. Proton Beam

The duoplasmatron source operates with a 2-A discharge. The extraction hole is 0.2 mm in diameter; the ion beam is accelerated by an extracting electrode negatively biased and decelerated by a ground potential electrode which is also the first electrode of the einzel lens. The beam energy spread is 5 eV. The ion beam is mass analyzed by a 90° deflection magnet and the outgoing proton beam is collimated by two diaphragms, 2 and 1.5 mm in diameter, separated by a drift distance 76 cm long. The geometrical beam divergence is 0.13°. A system composed of four pairs of deflection plates adjusts the beam alignment through the apparatus so that the beam transmission is never lower than 0.80 on the single-collision domain. A typical initial proton intensity is 10^{-8} A.

C. Cesium Cell

The cesium cell (Fig. 2) is made of pure copper. It is composed of a thick cylindrical boiler 20 mm in diameter, 60 mm high, and a cylindrical collision chamber 80 mm in diameter, 75 mm high, situated just above the boiler. The 2-g cesium reservoir is heated by alternating current in a resistance coil. A thermistor probe, connected to a Fenwall 500 proportional controller, can ensure a 0.1 °C regulation of the reservoir temperature, which is adjustable and measured by a thermocouple embedded into the copper wall in such a fashion that the thermocouple is within 2 mm of the liquid cesium. The thermocouple is connected to a compensating coil and was calibrated to within 0.2 °C with a mercury thermometer. The thickness of the boiler wall (15 mm) eliminates any measurable residual overshoot or undershoot around the control temperature point. The cesium temperature is known therefore with a 0.3 °C error. For a cesium temperature of 100 °C, the resulting error in the density is 3%.

Three more independent heating coils make the collision chamber temperature homogeneous and regulated within 1 °C as measured by the influence of the chamber temperature on the cesium vapor density, discussed in Sec. IID. A water-cooling tube can quickly reduce the cell temperature and recondense the cesium into the boiler.

The cell is filled with cesium under vacuum through a rotating stopper. Before being filled, the inner surface of the cell is polished by electrolysis. The ion beam enters the chamber through the 1.5-mm gold surface diaphragm. Two copper tubes 7 mm in diameter and 28 mm long, followed by two Freon-cooled traps, protect the experimental

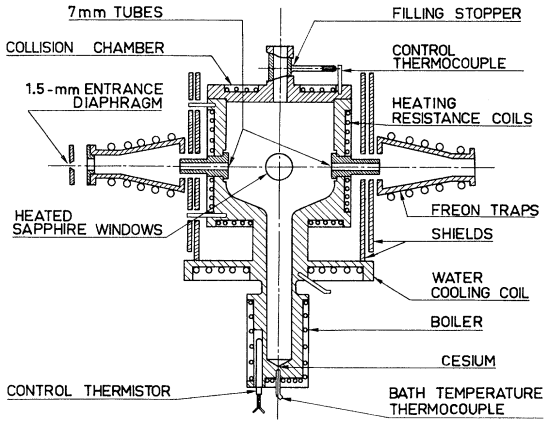

FIG. 2. Scaled drawing of the cesium cell. The cell is made of pure copper. The temperature of the boiler, which contains 2 g of cesium, is controlled and adjustable. The vapor density is measured by the absorption of the resonant light emitted by a cesium spectral lamp. The light beam enters and leaves the cell by means of two sapphire windows heated 20° higher than the boiler in order to avoid any condensation. The traps are Freon cooled at −40 °C to protect the apparatus from pollution.

setup from any cesium pollution. The effective length of the collision chamber is 103 mm, taking into account the tubes where the vapor density is supposed to vary linearly. The initial proton intensity I_+^0 is measured by a movable Faraday cup situated just behind the entrance diaphragm.

D. Measurement of Cesium Vapor Density

The measurement of the cesium vapor density must be carefully done so as to be sufficiently accurate and reproducible to not cause a major uncertainty in the cross sections of interest.

The saturated vapor pressure of cesium is known from the work of Taylor and Langmuir[24] who have used a surface ionization gauge to measure the vapor density. Their results have been later verified by Marino *et al.*,[25] Rozwadowski and Lipworth,[26] and this laboratory.[27] These measurements agree with the Langmuir-Taylor formula, used in Fig. 3, which is believed to be accurate to within 5% as long as thermodynamic equilibrium is carefully achieved. Furthermore, considerable care must be exercised so as to not contaminate the gauge with cesium.

In the present experiment it is clear that equilibrium is not well achieved when the boiler temperature is continuously varying as is necessary during a cycle of measurements. We have therefore chosen to use, as a relative parameter, the absorption of resonant cesium light by the cesium vapor. The absorption is instantaneous, reproducible, and independent of slight deviations from equilibrium. An ac-operated gas-discharge lamp (Philips E 27.0C) radiates the resonant cesium light $6P_{3/2}$-$6S_{1/2}$ (8521 Å) selected by an interference filter (MTO Intervex) which has a bandpass of 120 Å and a maximum transmission 0.41. The infrared light is focused into a parallel beam by a lens system and then crosses the cesium cell through two heated sapphire windows situated on a diameter perpendicular to the beam axis. The temperature of the windows is 20 °C higher than the boiler temperature in order to avoid condensation of Cs. Absorption of the light occurs in the vapor while the remaining flux strikes the photocathode of a RTC 150 CVP infrared photomultiplier which exhibits a maximum quantum efficiency (0.3%) at 8000 Å. The dark current of the detector is negligible compared to the collected signal. With a 0.9-A discharge current in the spectral lamp, the full width at half-maximum of the emitted resonance line is large enough (5 Å) to ensure nontotal absorption of the light up to a cell vapor density as high as 10^{14} atoms/cm^3 (140 °C) as shown in Fig. 3.

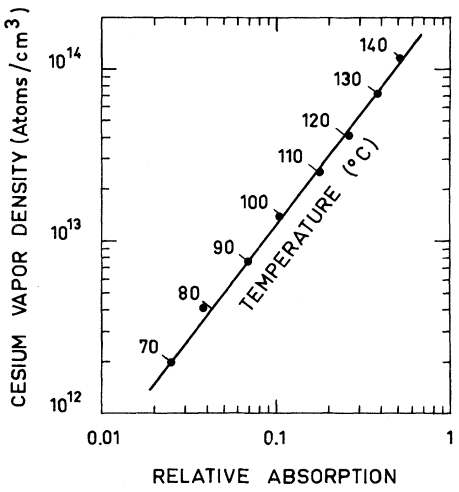

FIG. 3. Calibrated cesium vapor density as a function of the relative absorption of the resonant light $6P_{3/2}$-$6S_{1/2}$ (8521 Å) of cesium. The curve is calibrated by comparison with Langmuir-Taylor values of saturated vapor pressure vs temperature (Ref. 24): $\log_{10}P = 11.0531 - 1.35\log_{10}T - 4041/T$, with p in Torr and T in °K. Two calibration points, where thermodynamic equilibrium is carefully achieved, are used: 72 and 109 °C. The absorption is not total for temperatures as high as 140 °C, because the emitted resonant line has a 5-Å full width at half-maximum.

No theoretical assumption is made as to the dependence of absorption with cesium vapor density as we normalize the absorption to the Langmuir-Taylor results. The calibration procedure is as follows.

(a) The absorption of resonant cesium light is measured as a function of the boiler temperature. Each point on this curve is plotted when the cesium cell temperatures are regulated. The absorption is measured with an uncertainty of 1% and the photomultiplier current varies 4%.

(b) The influence of a variation of the collision chamber temperature has been tested. A 10 °C variation of the chamber temperature causes a 5% variation of the absorption when the boiler temperature is kept constant and less than the chamber temperature. The temperature of the windows does not appreciably affect the absorption. We have thus verified that the cesium vapor density essentially depends only upon the temperature of the coldest point of the cell, which is here the boiler. As the chamber temperature can be regulated to within 1 °C, the resulting error in the cesium density is about 2%.

(c) We have verified that the absorption does not change appreciably during several hours of regulation at two temperatures: 72 and 109 °C.

(d) By using the Langmuir-Taylor formula the cesium vapor density is plotted versus the absorption values as in Fig. 3. The total error in cesium density measurement, taking into account the 5% error of Langmuir formula, is about 15%.

(e) The shape of the emission line changes slowly with time as the spectral lamp becomes older. Therefore, the gauge is recalibrated every 2 weeks.

E. Quantitative Detection of Metastable Atoms

At the exit of the cesium cell the residual H^+ ions and the created H^- ions are swept away by a weak transverse electric field applied between two parallel plates 45 cm long and 2 cm apart. The remaining neutral beam contains the metastable hydrogen atoms together with unwanted ground-state atoms coming from the decay of the $2P_{1/2}$ and $2P_{3/2}$ radiative states.

The presence of an electric field reduces the lifetime of the metastable atoms according to the first approximation formula

$$t = (3.62 \times 10^{-4})/E^2 \ ,$$

where t is in sec and E in V/cm. At 2.5 keV, a 2.3-V/cm field strength is sufficient to remove all the ions from the beam. With such a field, only a 1.5% of the metastable atoms are quenched by Stark effect.

In this experiment the metastable atoms are quantitatively detected by applying a strong transverse electric field in order to induce Stark mixing between the $2S_{1/2}$, $2P_{1/2}$, $2P_{3/2}$ states, followed by the emission of Lyman-α photons which are then counted.

The quench field is applied between two plates 65 mm long and 40 mm wide biased at opposite potentials with respect to ground. The fringe fields are reduced by means of a set of image plates located 3 mm outside the inner plates. This ensures that the quenching of the metastable atoms occurs in a very small region in front of the detector. A plot of the field lines, obtained by simulation [Fig. 4(a)] shows that the fringe field is very small when the outer plates are 4 mm longer than the inner plates. In this case a zero-field point appears on the axis of the beam 25 mm before the edge of the plates.

The detector is a Bendix 762 uv channeltron which is essentially operating in a counting mode so that the counting rate N is fairly insensitive to the gain once a sufficient gain level is attained. The detector was precalibrated by means of a NO ionization chamber. Its quantum efficiency ($\eta = 0.107$) is maximum for Lyman-α wavelength. The photocathode diameter is 1.3 cm. The detector is fixed on an axial cylinder at ground potential which can move parallel to the beam and rotate around the axis of the beam without perturbing the electric quenching field. All the surfaces are cadmium coated to minimize reflection of photons. Efficiency of the cadmium coating was tested by removing the cylinder in front of the detector and verifying that no change occurred in the

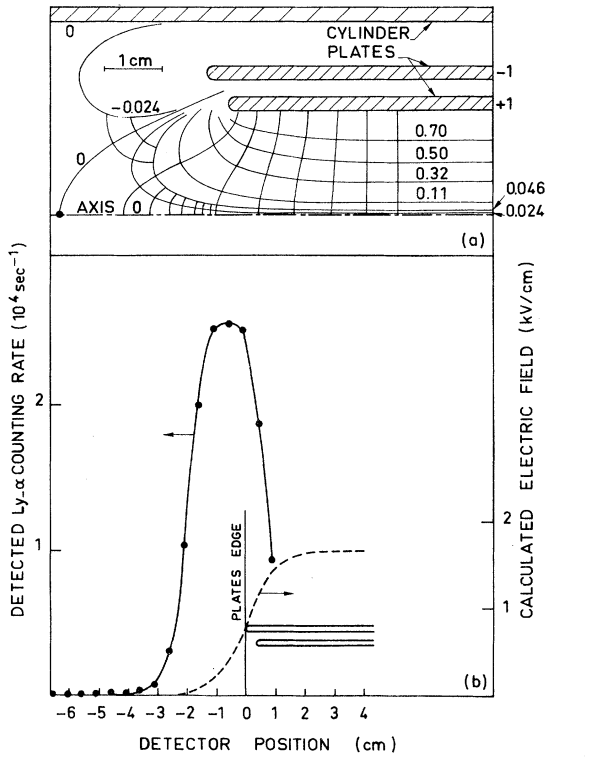

FIG. 4. Metastable atom-detection apparatus. (a) Cross section of the quenching apparatus (× 2). The axis of the beam is at the bottom of the figure. The potential lines are obtained by simulation. One notes that a zero potential line crosses the axis 25 mm before the edge of the longer plate, thus greatly reducing the fringe fields. (b) Solid line: detected photon counting rate when moving the detector parallel to the beam axis with the plates biased at ± 3000 V. The photocathode of the Bendix 762 detector is 74 mm from the axis, its diameter is 13 mm. The detector is perpendicular to the plane of the figure. Dash line: calculated electric field on the axis of the beam for ± 3000-V bias potentials.

counting rate under the same conditions. The reflectivity of an evaporated cadmium film is known to be about 1% at the Lyman-α wavelength.[28] Figure 4(b) shows that the detected signal increases very rapidly when moving the detector parallel to the axis of the beam towards the plates. The effective emitting section of the beam is not longer than 7 mm so that all the quenched atoms are within the view of the detector. When a potential of ± 3 kV is applied to the plates the calculated electric field is about 450 V/cm in this region.

In order to verify that the detected signal is only due to the quenching of the metastable atoms, the quench field is kept constant while the electric field E_p, applied between the sweeping plates, is increased. One can calculate the fraction of the metastable atoms which is prequenched. The remaining metastable fraction reaching the quench-

ing region can be written

$$f = e^{-kE_p^2} ,$$

where k is a constant which depends upon the energy of the beam and the geometry of the plates. It appears that the detected signal, when varying E_p, fits this formula when the correct value of the constant is used (Fig. 5). When $E_p = 50$ V/cm the detected signal is as low as 1% of the normal signal.

Thus, knowing the solid angle ($\Omega = 2.33 \times 10^{-2}$ sr) of the detector photocathode viewed from the emitting beam section, the cross section for the formation of the metastable atoms can be calculated in the case of a single collision process

$$\sigma_{+m} = 4\pi Ne/\Omega\eta I_+^0 \Pi_{Cs} ,$$

where N is the counting rate of the detector, η its quantum efficiency, I_+^0 is the entering proton intensity, and Π_{Cs} is the thickness of the cesium target. Care was taken that no appreciable loss or gain of metastable hydrogen atoms occurs. Thus destruction due to stray-field quenching was prevented by complete shielding of the beam from high-voltage conductors. The possibility of metastables being destroyed or created by collisions with background gas was shown to be negligible by demonstrating independence of the signal with background pressure. Care was taken to ensure that no metastable atoms were lost at the entrance aperture of the detection chamber by varying its diameter. Finally, signal loss occurring in the pulse-handling electronics was estimated to be negligible from the derivative of the curve of counting rate vs discriminator voltage.

By rotating the detector around the axis of the beam it is possible to take into account any inhomogeneity of the emission due to the polarization of the Lyman-α radiation.

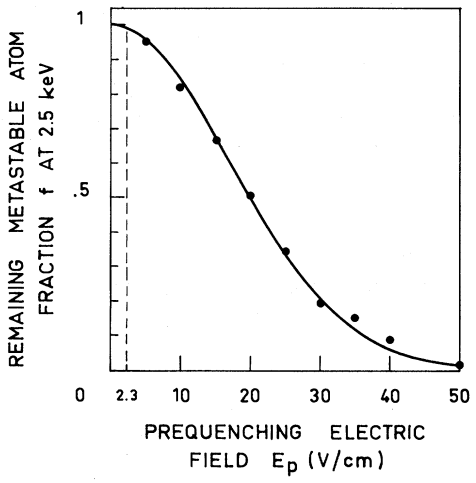

FIG. 5. Experimental evidence of an accurate detection of the metastable atoms. When prequenched by an electric field E_p applied between the sweeping plates, the metastable atoms show a remaining fraction $f = e^{-kE_p^2}$, where $k = 1.735 \times 10^{-3}$ is a geometric constant. This fraction can be quenched. Solid line: calculated curve using the formula above; closed circles: experimental quenched fraction. The agreement is excellent. The permanent sweeping field, removing the unwanted ions from the beam when measurements occur, is 2.3 V/cm. Thus more than 98.5% of the metastable atoms are transmitted.

F. Target Gas Cell

After leaving the Lyman-α detector chamber, the neutral beam enters the second cell containing the selected target gas where the metastable atoms undergo collisional destruction. At 2.5 keV, the main channels of this destruction are electron loss, electron attachment, and deexcitation. The positive and negative hydrogen ions created are separated by a magnetic field and quantitatively detected by Faraday cups. The entrance and exit diaphragms of the gas cell are adjustable and are sufficiently large so as to not attenuate the beam. The effective length of the cell is 26.2 cm.

Because the beam contains ground-state atoms together with metastable atoms, it is necessary to make two measurements: the first with nonquenched metastable atoms, and the second with all the metastable atoms quenched in the Lyman-α detector chamber. The ratio of the two cross sections for metastable and ground state is deduced from these measurements without using the absolute gas target thickness.

III. DATA

A. Cross Section for Formation of All Neutral States of Hydrogen

In a previous paper[29] the mechanism of the reaction of a proton beam interacting with cesium vapor was studied by measuring the negative ions H^- and the neutral particles H^0 outgoing intensities. The cross sections σ_{+0}, σ_{+-}, σ_{-0}, and σ_{0-} are given at 2.5-keV energy.

These measurements are extended here to the energy range 0.5–2.5 keV, for the attenuation of the proton beam in cesium vapor. Typically, at 2.5 keV and for a cesium vapor thickness $\Pi_{Cs} = 2 \times 10^{15}$ atom/cm^2, about 95% of the primary proton beam intensity is attenuated.

The cross section σ_{+0} for the production of all the neutral states of hydrogen increases slightly with decreasing energy as shown in Fig. 6 and is consistent with previous measurements of Schlachter *et al.*[4] The theory of Rapp and Francis[30] for nonresonant charge-exchange process ($\Delta E = 0.5$ eV) is represented on Fig. 6. The theoretical curve is normalized at 2.5 keV to our experi-

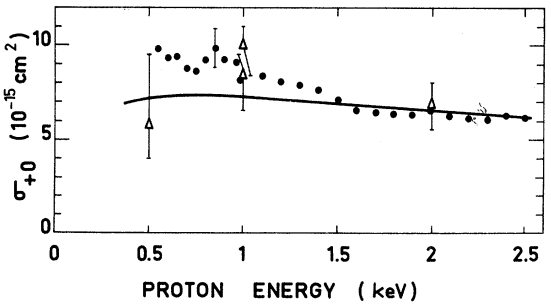

FIG. 6. Cross section σ_{+0}, in units of 10^{-15} cm^2, for the formation of all the neutral states of hydrogen in proton-cesium charge-exchange process. Open triangles: Schlachter *et al.* (Ref. 4); closed circles: present work; solid line: Rapp and Francis theory (Ref. 30) normalized to our experimental value at 2.5 keV.

mental point. The slope of the increasing curve for decreasing energy is consistent with experimental points between 2.5 and 1.5 keV. The theoretically predicted maximum at an energy 0.77 keV has not been observed, although Schlachter's measurement with deuterium ions at an effective energy 0.5 keV seems to indicates a maximum in the cross section.

B. Polarization of Lyman-α Radiation

The polarization of Lyman-α radiation emitted by metastable H(2S) atoms in an electric field has been previously discussed by Lichten,[31] Ott *et al.*,[5] Sellin *et al.*,[6] and Crandall[7] and is of practical importance since electric field quenching of H(2S) atoms is often used to determine a cross section for the production of H(2S) atoms. In this study, use was made of the fact that the Lyman-α radiation from the quenched 2S state is an electric dipole radiation. Thus the angular distribution is

$$I(\theta) = I_{\parallel} \sin^2\theta + I_{\perp}(1+\cos^2\theta) \ ,$$

where θ is the angular position relative to the quenching electric field and $I_{\parallel}$ and $I_{\perp}$ are the radiation intensities with electric field vector parallel and perpendicular to the quenching electric field when $\theta = 90°$. The first term of this equation describes contributions of transitions with $\Delta M = 0$, the emitted light being linearly polarized (M is the azimuthal quantum number). The second term arises from transitions with $\Delta M = \pm 1$, the emitted light being elliptically polarized.

Introducing the polarization fraction P defined by

$$P = (I_{\parallel} - I_{\perp})/(I_{\parallel} + I_{\perp}) \ ,$$

the angular distribution of the Lyman-α radiation can be written as

$$I(\theta) = \frac{3I_0}{4\pi} \frac{1 - P\cos^2\theta}{3 - P} \ ,$$

where I_0 is the total intensity of emitted radiation.

Thus the polarization fraction was determined from measurements of $I(90°)$, $I(0°)$, and $I(180°)$, where the criterion for acceptability of data was that $I(0°) = I(180°)$ as required by symmetry of electric dipole radiation. Then P is calculated with the formula

$$P = [I(90°) - I(0°)]/I(90°)$$

for different electric field strengths.

It has recently been shown that the field-induced Lyman-α emission is polarized by an amount which varies with field strength.[6,7] The measured radiation polarization is $P = -0.31 \pm 0.03$ for weak quench electric field ($E < 100$ V/cm) in agreement with previous measurements of Ott *et al.* who found -0.30 ± 0.02 by using a different method.

When the quench electric field is increasing it appears that the polarization tends to zero. Up to now it has not been possible with our quenching system to obtain accurate measurements of P for strong quench fields because the electric field is not constant in the region, viewed by the detector, where radiation occurs. A new quenching system has to be used.

C. Cross Section for Formation of Metastable Atoms: Percentage of Metastable Atoms

As the cesium target thickness Π_{Cs} increases, one notes a linear decrease of the proton intensity I_+ (Fig. 7). Simultaneously the metastable atom intensity I_m increases linearly. Simple collisions occur and the slope of the linear part of the inten-

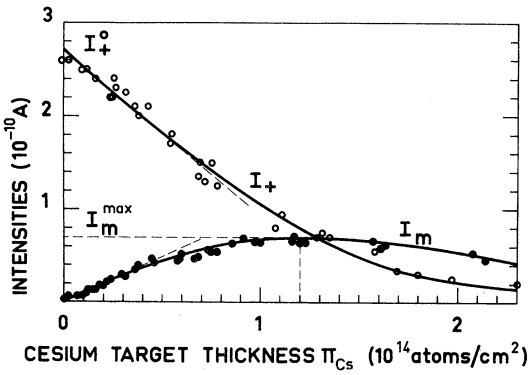

FIG. 7. Measured intensities at the exit of the cesium cell as a function of the cesium target thickness, at 2.4 keV. Open circles, proton intensity I_+; closed circles, absolute metastable atom intensity I_m (× 2). The slope of the linear part of the curve I_m is determined by a least-squares method and gives the cross section for the formation of metastable atoms in proton-cesium charge-exchange process $\sigma_{+m} = 1.7 \times 10^{-15}$ cm^2. The percentage of metastable atoms in the outgoing neutral beam is the ratio $\sigma_{+m}/\sigma_{+0} = 0.27$. The absolute maximum I_m^{max} of the curve I_m is a 0.13 fraction of the initial proton flux I_+^0.

sity I_m gives the cross section σ_{+m} for the formation of the metastable atoms. Our measured value of σ_{+m} at 2.4 keV is compared with previous measurements in Table I.

The agreement with Donnally's result is reasonable when one takes into account all the sources of error. The cesium target thickness is measured with a 15% error. Calibration of the Lyman-α detector gives a 5% error in quantum efficiency. The solid angle of the photocathode can vary about 5% when the beam is slightly disaligned. The slope of the linear part of the I_m curve is known with a 5% error, and the initial proton flux I_+^0 varies about 5%. So the cross section σ_{+m} is measured with a 35% error. Nevertheless, the discrepancy with Cesati's result is not understood. The high value of Sellin's result is probably due to a wrong normalization on Il'in's measurements of the total cross section for the formation of all the neutral states at 10 keV.[32]

The ratio of the cross sections σ_{+m} and σ_{+0} gives the percentage F of metastable atoms in the neutral beam. We obtain the value $F = 0.27$ for small cesium target thickness. Until now the most frequently assumed value has been $F = 0.25$, which is slightly less than our measured value. Furthermore it appears in Fig. 7 that the ratio F decreases with increasing target thickness. When Π_{Cs} is greater than 10^{13} atoms/cm^2, multiple collisions are not negligible and the metastable atoms can be destroyed by these collisions on cesium. The intensity I_m continues to increase nonlinearly with Π_{Cs} up to a maximum for a thickness of $1.2\ 10^{14}$ atoms/cm^2. At the maximum, the ratio of the intensity I_m to the initial proton intensity is 0.13, which is the maximum proton fraction that this charge-exchange process can transform into metastable atoms at 2.4 keV. In view of the value of 0.0021 for the equilibrium value of the proton fraction at 2 keV as measured by Schlachter *et al.*,[4] this maximum in the intensity I_m probably indicates the influence of collisional quenching of the metastable atoms with a large value of the cross section σ_{mg}.

D. Electron Loss and Electron Attachment of Metastable Hydrogen Atoms

The collisional destruction of metastable hydrogen atoms is a complex process involving deexcitation, excitation, electron loss, and negative-ion formation. Both experimental and theoretical data on either the total destruction cross section or on the individual cross sections which contribute to the total destruction are still very limited, especially below 10 keV.

One assumes that for the 0.5–2.5-keV energy range the following three processes,

TABLE I. Measured value of σ_{+m} at 2.4 keV compared with previous measurements.

Author	σ_{+m} (Experiment) (cm^2)
Donnally *et al.* (Ref. 1)	3.5×10^{-15}
Cesati *et al.* (Ref. 2)	8×10^{-17}
Sellin and Granoff (Ref. 3)	2×10^{-14}
Present work	1.7×10^{-15}

$$\mathrm{H}(2S)+X \rightarrow \begin{cases} \mathrm{H}^+ + X + e & (\sigma_{m+}) \text{ electron loss} \\ \mathrm{H}^- + X^+ & (\sigma_{m-}) \text{ electron attachment} \\ \mathrm{H}(1S) + X + \text{Ly-}\alpha & (\sigma_{mg}) \text{ deexcitation} \end{cases},$$

may give appreciable contributions to the total destruction cross section for metastable hydrogen atoms.

In this section, determinations of the electron-loss cross section σ_{m+} for collision with noble gases H_2, N_2, and HI are presented. The electron attachment cross section σ_{m-} is given for N_2.

Let us denote by the indices g, m, and + the states H(1S), H(2S), and H^+, respectively. If F is the percentage of neutral atoms which enter the gas target in the metastable state, one can determine σ_{m+}/σ_{g+} by measuring the positive-ion intensity leaving the second gas target for two known values of F. If I is the total neutral intensity, composed of an intensity I_m of atoms in the 2S state and I_g in the ground state, the intensity I_+ of protons created in the gas target with a thickness Π, low enough to ensure single collisions, will be

$$I_+ = I[F\sigma_{m+} + (1-F)\sigma_{g+}]\Pi ,$$

where $F = I_m/I$ and $I = I_m + I_g$.

When all the metastable atoms are quenched before entering the gas cell, the newly created proton intensity I_+' is

$$I_+' = I\sigma_{g+}\Pi .$$

Thus one obtains

$$\sigma_{m+}/\sigma_{g+} = (R-1)/F + 1 ,$$

where $R = I_+/I_+'$.

The ratio of the two cross sections is independent of the target thickness Π. Knowing R, F, and σ_{g+}, it is possible to deduce the electron-loss cross section for the metastable state of hydrogen. To detect sufficient proton intensities, a thick cesium target is used, for which the metastable atom intensity I_m is maximum. At this maximum, the percentage of metastable atoms ($F = 0.16$) is important enough to neglect the effect of the small fraction of highly excited states of hydrogen created in the cesium cell by nonresonant charge exchange. The cross sections σ_{g+} for all gas targets except N_2 and HI are obtained from the paper

of Williams[20] who summarizes most of the literature on this subject and has measured the electron-loss cross section of ground state of hydrogen down to 2 keV. The discrepancy with previous measurements of Stier and Barnett, [33] in the energy range 4–50 keV, is not larger than 25% for a molecular hydrogen target and 20% for noble-gas targets. For N_2, the two cross sections σ_{g+} and σ_{m+} are separately measured, and for HI no value of σ_{g+} has been found in the literature.

Figure 8 displays a typical increase of I_+ and I_+' versus Π in the case of helium. One notes the nonlinear increase of the intensities for thick gas targets, especially when metastable atoms are contained in the beam.

Table II shows measured values of R and σ_{m+}/σ_{g+}. Using the value of σ_{g+}, one obtains the cross section σ_{m+} which is compared with the theoretical prediction of Bates[14,15] who calculated σ_{m+} by a classical impulse approximation based on a structureless model. For N_2, Ar, and Kr the theoretical values are too high by factors equal to 1.7, 1.4, and 2.2, respectively. The discrepancy is the most important for the heaviest gas target, according to a general feature of this kind of approximation. Furthermore our values of σ_{m+} for N_2, Ar, and Kr are consistent with extrapolated results of Gilbody *et al.*[13] who worked in the energy range 10–30 keV where the discrepancy with theory is of the same order. For the light gas targets He and Ne, the discrepancy is inversed while the

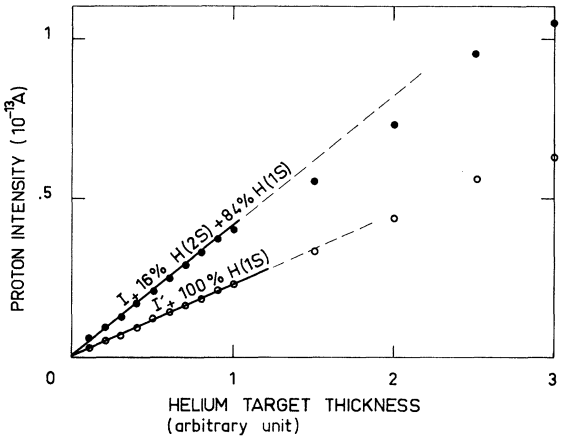

FIG. 8. Ratio of the electron-loss cross sections between metastable and ground states of hydrogen atoms in collisions with a helium target at 2.5 keV. Closed circles: created photon intensity I_+ as function of target thickness (in arbitrary units) when the incoming neutral beam contains 16% of metastable atoms. Open circles: proton intensity I_+' for the same conditions when all the metastable atoms are quenched before reaching the target. The ratio between the slopes of the two linear parts is $R = 1.82$ and gives the cross section ratio $\sigma_{m+}/\sigma_{g+} = 5.9$.

TABLE II. Ratio of the electron-loss cross sections between metastable and ground-state atoms of hydrogen on different gas targets. The reference cross section σ_{g+}, in units of 10^{-17} cm^2, is from Williams, except for nitrogen for which σ_{g+} is measured. The obtained values of σ_{m+}, in units of 10^{-16} cm^2, are compared with theoretical calculation of Bates, using a classical impulse approximation based on a structureless model.

Target gas	R	$\frac{\sigma_{m+}}{\sigma_{g+}}$	σ_{g+} (10^{-17} cm^2) (Ref. 20)	σ_{m+} (10^{-16} cm^2) Expt.	Theory (Refs. 14 and 15)
He	1.82	5.9	7	4.1	1.7
Ne	1.47	3.8	7	2.7	1
Ar	1.43	3.6	8	2.9	4
Kr	1.40	3.4	8	2.7	6
Xe	1.50	4	15	6	
H_2	1.97[a]	6.8	5	3.4	
N_2	1.78	5.9	8.5[b]	5[b]	8.5
HI	2.74	9.7			

[a]Donnally *et al.* (Ref. 34), 1.9.
[b]Absolute measurement.

measurements of Gilbody *et al.* between 10 and 30 keV are in excellent agreement with the theory. The comparisons above are somewhat reduced if one takes into account the errors of the measurements. The percentage F is known with a 35% error and the values of σ_{g+} at 2.5 keV in the literature vary about 20–25% according to the author.

For all the gas targets the electron-loss cross section is greater with the metastable atom than with the ground-state hydrogen atom. This feature is very important for the halogen compound target HI which gives $R = 2.74$ and $\sigma_{m+}/\sigma_{g+} = 9.7$.

With a molecular iodine target, Knutson[23] has found, at 2.5 keV, the following close results $R = 2.2$ and $\sigma_{m+}/\sigma_{g+} = 5.8$.

As pointed out by Brückmann *et al.*, [21] the large value of σ_{m+}/σ_{g+} for halogen compound targets can be explained by their electron affinity which is close to the ionization energy of metastable hydrogen (3.4 eV). The electron affinity of atomic iodine is 3.2 eV. Thus HI can be used as a selective target to ionize the metastable hydrogen atoms in a beam containing the two species H(2S) and H(1S).

As for electron attachment of metastable hydrogen, the only available result is for a nitrogen target. The two cross sections σ_{g-} and σ_{m-} are separately measured at 2.5 keV for the reaction

$$H(1S, 2S) + N_2 \rightarrow H^-(1s^2) + N_2^+ ,$$

$$\sigma_{g-} = 9.7 \times 10^{-18} \text{ cm}^2, \quad \sigma_{m-} = 1.2 \times 10^{-16} \text{ cm}^2 .$$

The cross section is surprisingly high for the metastable state.

ACKNOWLEDGMENTS

The authors are grateful to Dr. C. Manus and G. Watel for their helpful assistance and to Dr. B. L. Donnally for several useful conversations.

[1]B. L. Donnally, T. Clapp, W. Sawyer, and M. Schultz, Phys. Rev. Letters 12, 502 (1964).
[2]A. Cesati, F. Cristofori, L. Millazo Colli, and P. G. Sona, Energia Nucl. (Milan) 13, 649 (1966).
[3]I. A. Sellin and L. Granoff, Phys. Letters 25A, 484 (1967).
[4]A. S. Schlachter, P. J. Bjorkholm, D. H. Loyd, L. W. Anderson, and W. Haeberli, Phys. Rev. 177, 184 (1969).
[5]W. R. Ott, W. E. Kauppila, and W. L. Fite, Phys. Rev. A 1, 1089 (1970).
[6]I. A. Sellin, J. A. Biggerstaff, and P. M. Griffin, Phys. Rev. A 2, 423 (1970).
[7]David H. Crandall, thesis (University of Nebraska, 1970) (unpublished).
[8]V. Dose, V. Meyer, and M. Salzmann, J. Phys. B 3, 135 (1969).
[9]F. W. Byron, Jr., R. V. Krotkov, and John A. Medeiros, Phys. Rev. Letters 24, 83 (1970).
[10]R. V. Krotkov, F. W. Byron, J. A. Medeiros, and K. M. Wang, Phys. Rev. (to be published).
[11]F. W. Byron, Jr. and J. I. Gersten, Phys. Rev. A 3, 620 (1971).
[12]H. Levy II, Phys. Rev. A 3, 1987 (1971).
[13]H. B. Gilbody, R. Browning, R. M. Reynolds, and G. I. Riddel, J. Phys. B 4, 94 (1971).
[14]D. R. Bates and J. C. G. Walker, Planetary Space Sci. 14, 1367 (1966).
[15]D. R. Bates (private communication).
[16]K. L. Bell and A. E. Kingston, J. Phys. B 4, 162 (1971).
[17]B. L. Donnally and W. Sawyer, Phys. Rev. Letters 15, 439 (1965).
[18]R. S. Kass and W. L. Williams, Phys. Rev. Letters 27, 473 (1971).
[19]R. A. Baragiola and E. R. Salvatelli, Phys. Rev. A 3, 514 (1971).
[20]J. F. Williams, Phys. Rev. 153, 116 (1967).
[21]H. Brückmann, D. Finken, and L. Friedrich, Phys. Letters 29B, 223 (1969).
[22]H. Brückmann, D. Finken, and L. Friedrich, Nucl. Instr. Methods 87, 155 (1970).
[23]L. D. Knutson, Phys. Rev. A 2, 1878 (1970).
[24]J. B. Taylor and I. Langmuir, Phys. Rev. 51, 753 (1937).
[25]L. L. Marino, A. C. H. Smith, and E. Caplinger, Phys. Rev. 128, 2243 (1962).
[26]M. Rozwadowski, and E. Lipworth, Phys. Rev. 43, 7 (1965); 43, 2347 (1965).
[27]P. Pradel, Mémoire du Conservatoire National des Arts et Métiers, 1972 (unpublished).
[28]L. R. Koller, *Ultraviolet Radiation* (Wiley, New York, 1965), p. 209.
[29]G. Spiess, A. Valance, and P. Pradel, Phys. Letters 31A, 434 (1970).
[30]D. Rapp and W. E. Francis, J. Chem. Phys. 37, 2631 (1962).
[31]W. Lichten, Phys. Rev. Letters 6, 12 (1961).
[32]R. Il'in, V. Oparin, E. Solov'ev, and N. Fedorenko, Zh. Eksperim. i Teor. Fiz. Pis'ma v Redaktsiyu 2, 310 (1965) [Sov. Phys. JETP Letters 2, 197 (1965)].
[33]P. M. Stier and C. F. Barnett, Phys. Rev. 103, 896 (1956).
[34]B. L. Donnally and W. Sawyer, in Sixth International Conference on the Physics of Electronic and Atomic Collisions, 1969 (unpublished).